Supplementary Material

Nanomorphology of Eco-Friendly Colloidal Inks, Relating Non-Fullerene Acceptor Surface Energy to Structure Formation

Matthew G. Barr[a], Sylvain Chambon[b,c], Adam Fahy[a], Timothy W. Jones[d], Matthew A. Marcus[e], A. L. David Kilcoyne[e], Paul C. Dastoor[a], Matthew J. Griffith,[a,f] Natalie P. Holmes[a,g]*

[a] Centre for Organic Electronics, University of Newcastle, Callaghan, NSW 2308, Australia

[b] University of Bordeaux, IMS, CNRS, UMR 5218, Bordeaux INP, ENSCBP, F-33405 Talence, France

[c] LIMMS/CNRS-IIS (UMI2820), Institute of Industrial Science, The University of Tokyo, 4-6-1 Komaba, Meguro-ku, Tokyo, 153-8505, Japan

[d] CSIRO Energy Centre, Mayfield West, NSW 2304, Australia

[e] Advanced Light Source, Lawrence Berkeley National Laboratory, Berkeley, CA 94720, USA

[f] School of Aerospace, Mechanical and Mechatronic Engineering, University of Sydney, Camperdown, NSW 2006, Australia

[g] Australian Centre for Microscopy and Microanalysis, University of Sydney, Madsen Building F09, NSW 2006, Australia

1. UV-Vis of Organic Semiconductor Materials
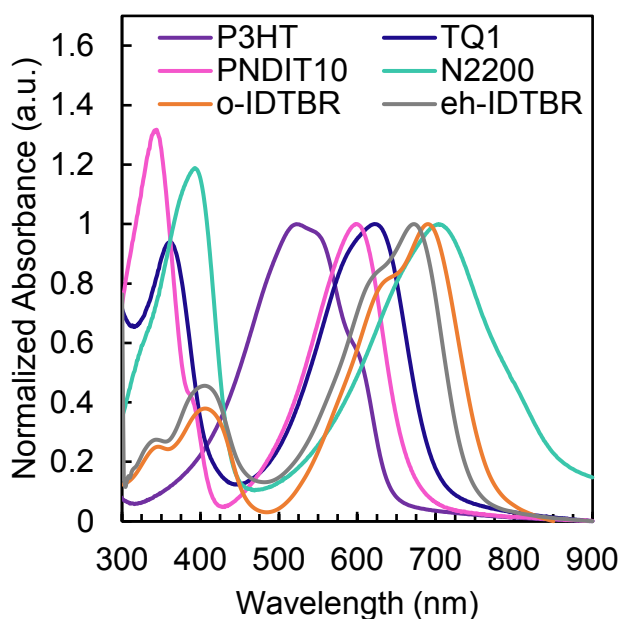
Figure S1. UV-Vis absorbance spectra of P3HT (purple), TQ1 (blue), PNDIT10 (pink), N2200 (green), o-IDTBR (orange) and eh-IDTBR (grey) films spin coated from chloroform solutions, without annealing. Absorbance normalized to peak height (long wavelength peak).
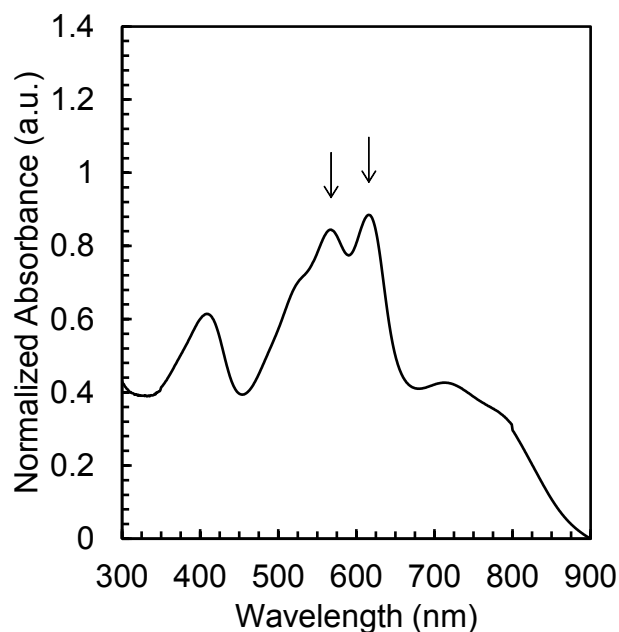
Figure S2. UV-Vis absorbance spectrum of P3HT:N2200 nanoparticle ink in quartz cuvette (dilution 1 in 60). Crystalline P3HT vibronic peaks are indicated with arrows.

2. Orthogonal Energy Selection Discussion

The NEXAFS spectra of the components of the polymer-donor: NFA samples tend to be much more similar than is typically the case for the more traditional systems incorporating fullerene-acceptors. This similarity is because (1) NFAs typically possess far fewer sp^2-bonding environments, leading to a diminished (or non-existent) C1s-pi* transition peak; (2) NFAs are often polymers, which offer up relatively similar chemistry to the polymer materials used as donor materials.

As a result of the NEXAFS spectra being much less distinct for polymer-donor:NFA blend systems, it can sometimes be advantageous to collect stacks with a greater number of orthogonal energies than the number of individual components. Provided that no photo-degradation of the blend films is observed (monitored by running NEXAFS spectra pre- and post-stack), collecting a denser stack allows for more combinations of energies to be trialed with SVD fitting. For example, collecting a three-energy stack yields four different combinations of orthogonal energies for the SVD analysis. Analysis of the stack is run for all of the combinations, with an aim to minimize the residuals from the resultant composition maps. The specific combination of orthogonal energies that produce the smallest residuals – that is those that lead to the best fit – are then used for all subsequent analysis of the blend system.

For a representative polymer-donor:NFA system – namely a 1:1 blend of P3HT and o-IDTBR – four different energies (284.1, 285.4, 287.7 and 291.0 eV) were trialled as the orthogonal set (Figure S3). Of these energies, only 285.4 eV could be considered an obvious candidate, utilizing a large difference in absolute absorption between the two components. 284.1 eV constitutes an energy typically categorized as pre-carbon K-edge (for amorphous carbon

materials), and offers up a situation whereby one component of the blend film has commenced absorbing at said K-edge, whilst the other component has not (to within the background absorption level). The disadvantage of using such a "pre-edge" energy is that the absolute absorption of even the "absorbing" component is very small, which can potentially lead to a lot of noise in the final stack analysis. On the other hand, whilst 291.0 eV does not appear as an obvious energy choice for component analysis, the very high absolute absorption at these higher "post-edge" energies lends itself to a relatively enhanced difference in signal for the two components. Although, note that if the difference in absorption for the two components at this energy is very small, this can also lead to more noise appearing in the final analysis, much as in the case for the pre-edge energy.

Table S1 lists the energies that were trialed for each of the six systems studied. Note that the energies highlighted in bold text indicate those chosen as the orthogonal set for analysis of the system. For clarity, a blue background indicates energies representative of the polymer donor, a red background shows those for the NFA, and a purple background specifies an energy that could be considered appropriate for both.
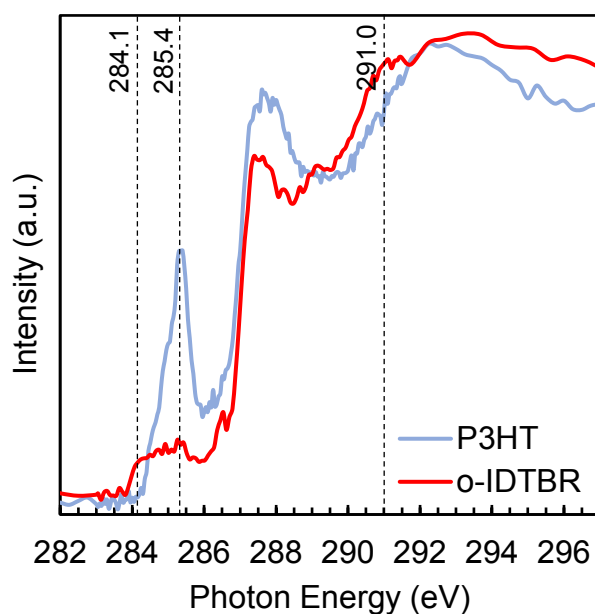
Figure S3. Overlaid spectra for the donor polymer P3HT (blue) and NFA o-IDTBR (red). Also shown are four analysis energies that have been utilized for the relative component analysis of the pristine materials comprising the blend film.

Table S1: Orthogonal energies trialed for each of the donor-polymer:NFA systems used in the study. Bolded values indicate those energies that produced the smallest residuals in the SVD analysis.

Donor:Acceptor System (Ratio)	Orthogonal Energies (eV)					
	Pre-edge					*Post-Edge*
TQ1:PNDIT10 (1:1)		**285.2**	286.2	**287.6**		291.6
TQ1:N2200 (1:1)	284.0	**285.2**	285.8	286.1	**287.8**	
TQ1:N2200 (2:1)	284.0	**285.2**	285.8	286.1	**287.8**	
P3HT:N2200 (1:1)		**285.4**	**285.8**	287.8		
P3HT:o-IDTBR (1:1)	284.1	**285.4**	287.7			291.0
P3HT:eh-IDTBR (1:1)	284.1	**285.4**				**291.0**

3. STXM Maps

STXM maps depicting a core-shell morphology for P3HT:eh-IDTBR nanoparticles synthesized via the miniemulsion method.
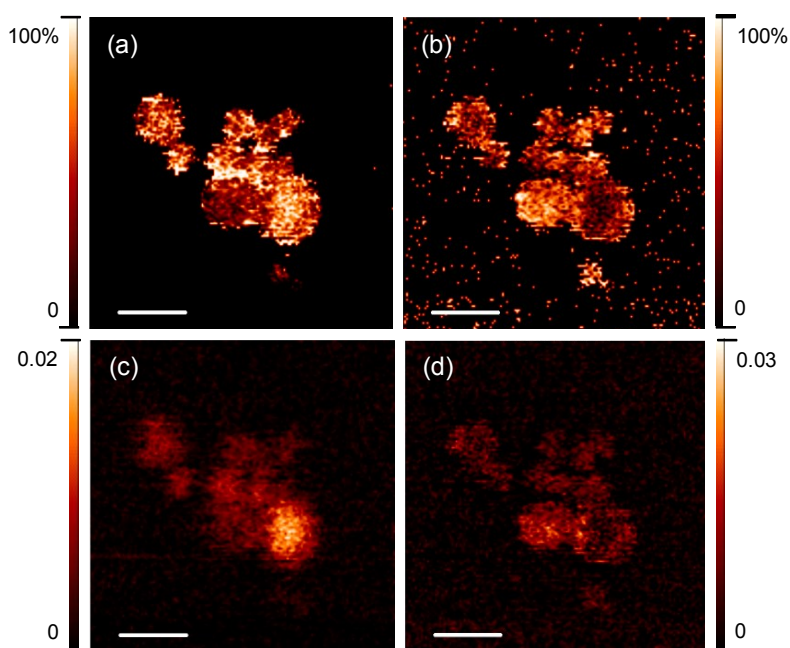
Figure S4. STXM fractional composition maps showing the concentration of (a) P3HT and (b) eh-IDTBR with corresponding STXM mass plots (c and d) for 1:1 P3HT:eh-IDTBR miniemulsion nanoparticles. All scale bars are 500 nm. The colour contrast is scaled such that light colours correspond to higher component concentrations. For the mass plots (c, d) the colour scale bars indicate concentration of component in mg cm^{-2}.

4. Method of Deriving Radial Profiles

The STXM fractional composition maps are first exported from the aXiS software as xyt files. Then MATLAB is used to replot the data, identify suitable nanoparticle regions for radial profiling, and for defining the centre coordinates and radius of nanoparticles. Nanoparticle radius is converted to units of nanometers based on the resolution of the original STXM map,

typically 1 pixel = 16 nm, but this is dependent upon the measurement setup for each map. MATLAB is then used to extract a radial profile (see example in Figure S5). This routine is performed for multiple nanoparticles, over a range of sizes, in each sample set.
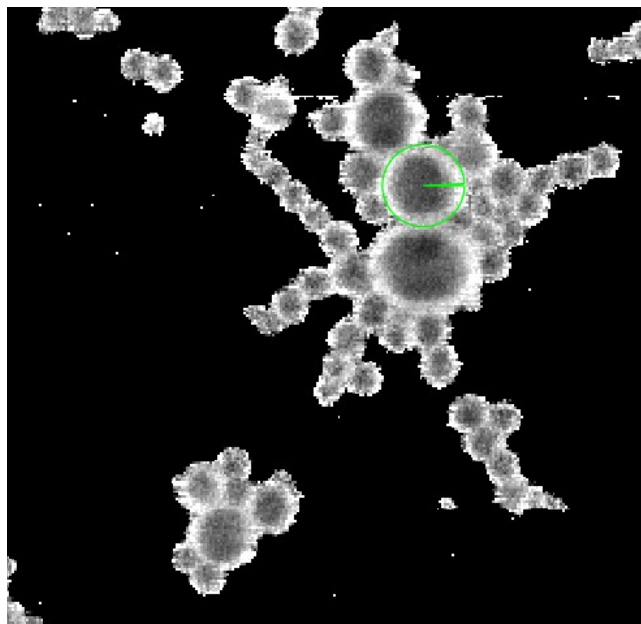
Figure S5. Radial profile extraction from a TQ1:PNDIT10 nanoparticle, matching the profile data plotted in Figure 5a.

5. Surface Energy Determination of PNDIT10

To characterize the surface energy of NFA PNDIT10, we used Fowkes' theory which splits the surface energy of a surface into dispersive and non-dispersive (polar) contributions. It is an extended theory beyond the empirical Zisman theory, which is appropriate for characterizing polymer surfaces with polar heteroatoms and/or functional groups, such as the naphthalene diimide/thiophene groups present in PNDIT10.[1]

Fowkes' theory derives from the work of adhesion of a solid|liquid interface and Young's equation. The liquid surface tension (γ_L) is separated into dispersive (d superscript) and polar (p superscript) components via geometric means. The surface energy contributions of the solid (γ_S) are separated similarly. Fowkes' theory gives;

$$\left(\gamma_L^d\right)^{1/2}\left(\gamma_S^d\right)^{1/2}+\left(\gamma_L^p\right)^{1/2}\left(\gamma_S^p\right)^{1/2}=\frac{\gamma_L\left(\cos\theta+1\right)}{2}, \tag{1}$$

where θ is the contact angle of a liquid on the polymer surface. To solve for the surface energy contributions, we use a reference liquid with no polar contributions to its surface tension. Diiodomethane is the standard practical reference liquid for this purpose (see Table S2). Elimination of the polar contributions towards Equation (1) gives;

$$\gamma_S^d=\frac{\gamma_L\left(\cos\theta+1\right)^2}{4}, \tag{2}$$

which for a contact angle of diiodomethane on PNDIT10 of 57.64 ° (see Figure S6a) gives a dispersive contribution of surface energy of $\gamma_S^d = 29.9$ mJ m^{-2}. We use water as a second reference liquid which has a mixed polar and dispersive contribution towards it surface tension. With the value for γ_S^d obtained above, only γ_S^p remains as unknown in Equation (1). With a contact angle of 102.45 ° (see Figure S6b) for water, we calculate the polar contribution to surface energy gives $\gamma_S^p = 0.2$ mJ m^{-2}.

The total surface energy of the solid (γ_S) is calculated using Equation (3);

$$\gamma_S = \gamma_s^p + \gamma_s^d$$

(3)

yielding a total surface energy of 30.1 mJ m^{-2} for PNDIT10.

Table S2. Surface tension dispersive (γ_L^d) and polar (γ_L^p) contributions for the test liquids[2] and their contact angle data on PNDIT10 polymer films (average of 3 measurements).

Contact Liquid	Surface Tension / mN m^{-1}			Contact Angle on PNDIT10, θ / °
	γ_L^d	γ_L^p	γ_L	
Diiodomethane	50.8	0.0	50.8	57.64
Water	21.8	51.0	72.8	102.45
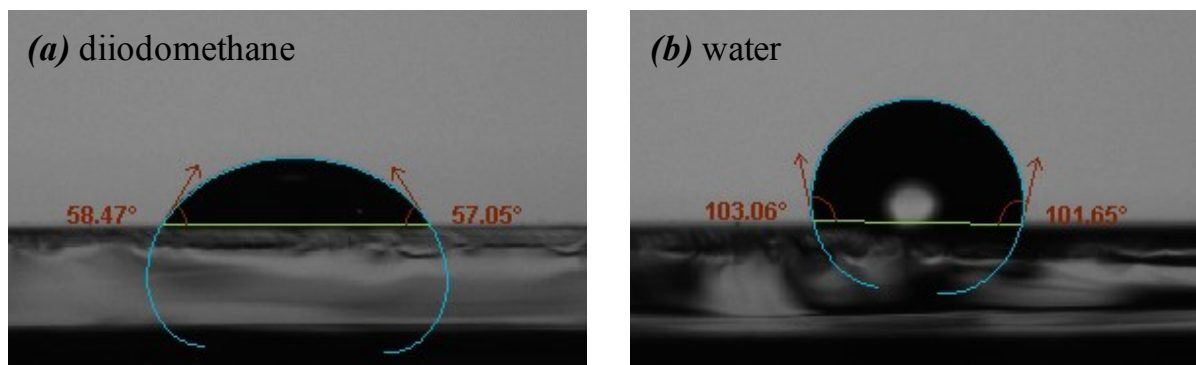
Figure S6. Contact angles of reference liquids (a) diiodomethane and (b) water on NFA polymer film PNDIT10.
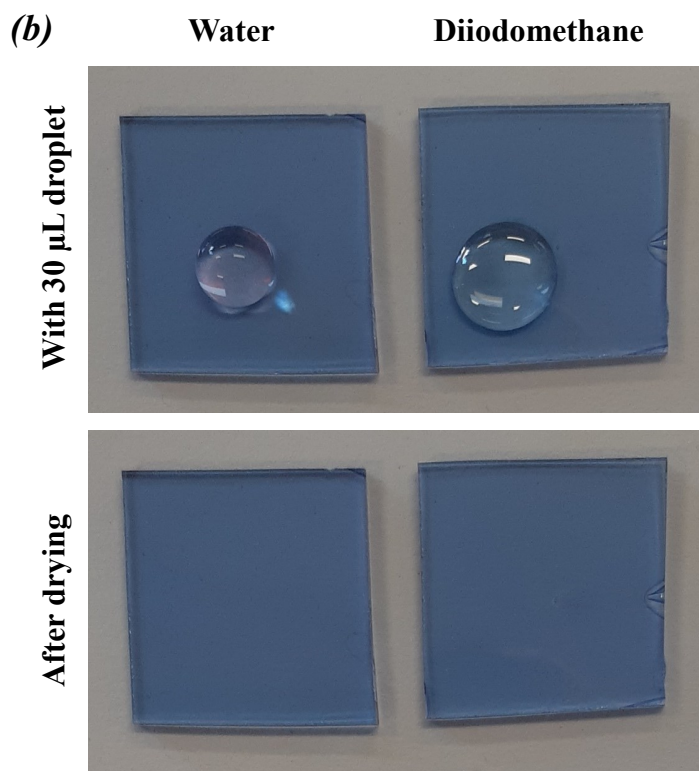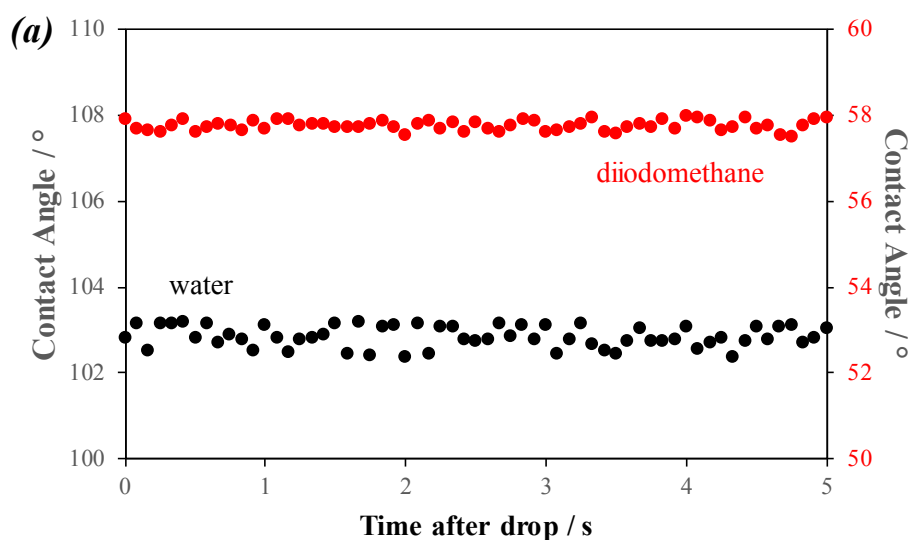
Figure S7. (a) Temporal data of contact angles of diiodomethane and water showing stable contact angles. (b) Images of film with 20 µL droplet applied for 30 s and after drying with a paper tissue and air dry showing no physical change to the film.

References:

(1)   Li, Z.; Xu, X.; Zhang, W.; Meng, X.; Ma, W.; Yartsev, A.; Inganäs, O.; Andersson, M. R.; Janssen, R. A. J.; Wang, E. High Performance All-Polymer Solar Cells by Synergistic Effects of Fine-Tuned Crystallinity and Solvent Annealing. *J. Am. Chem. Soc.* **2016**, *138*, 10935–10944.

(2)   van Oss, C. J. *Interfacial Forces in Aqueous Media*; Dekker: New York, 1994.